Theoretical investigation of a tunable free-electron light source

Shenggang Liu, Min Hu,* Yaxin Zhang, Weihao Liu, Ping Zhang, and Jun Zhou
Terahertz Research Center, University of Electronic Science and Technology of China, Chengdu 610054, China
(Received 9 December 2010; revised manuscript received 17 February 2011; published 30 June 2011)

The concept and experimental results of a light source given in a recent paper by Adamo *et al*. [Phys. Rev. Lett. **103**, 113901 (2009)] are very interesting and attractive. Our paper presents detailed theoretical investigations on such a light source, and our results confirm that the mechanism of the light radiation experimentally detected in the published paper is a special kind of diffraction radiation in a waveguide with nanoscale periodic structure excited by an electron beam. The numerical calculations based on our theory and digital simulations agree well with the experimental results. This mechanism of diffraction radiation is of significance in physics and optics, and may bring good opportunities for the generation of electromagnetic waves from terahertz to light frequency regimes.

DOI: 10.1103/PhysRevE.83.066609 PACS number(s): 42.72.−g, 41.60.−m, 42.25.Fx

I. INTRODUCTION

Recently, two very important and interesting papers were published [1,2], which present the concept of a light well and demonstrate experimental results. The schematic system is shown in Fig. 1 of [1]. It is a waveguide with nanoscale periodic structure, and an electron beam is injected into the cylindrical hole from the point of (r_0,θ_0) to excite light radiation. The system is made of gold, the diameter is 700 nm, the period is 400 nm, and there are six periods with SiO_2 filling in the gap. Tunable light radiation around a frequency of 400 THz with intensity of about 200 W/cm^2 excited by an electron beam with 20–40 keV was detected experimentally, and the lateral size of the structure is only a few hundred nanometers. Therefore, it is a very interesting and attractive proposal, and the experimental results are presented in these two papers. It is worth making further theoretical investigation as deep as possible, which is the goal of this paper.

A careful study of Ref. [1] revealed the following important points:

(1) Since the nanoscale periodic structure is made of gold and the operation wavelength is around 710 nm, the theoretical study and digital simulations should take surface plasmons (SPs) into account.

(2) The Brillouin diagram of the dispersion curve of Fig. 3 in [1] is expanded and shown in Fig. 1 of our paper. We can see there are five transverse electric (TE) and transverse magnetic (TM) modes presented: TE_{11}, TM_{01}, TE_{21}, TE_{01}, and TM_{11} modes (the last two modes are degenerate modes). The excitation is by a uniformly moving electron beam traveling along the axial direction, so only TM modes can be induced in the structure.

(3) The intersection points marked by a circle in Fig. 3 of [1] are the coupling points of the modes and beams. The frequencies of light radiation detected in [1] are close to that of the intersection points of the dispersion curve with the electron beam lines. Some of the points represent the backward waves, and others represent the forward waves. The detected radiation in the experiment of [1] should only be the backward waves.

(4) The experimental results are very interesting and important. However, it seems that there is no theoretical study on the mechanism of the light radiation generation, and that is the most significant problem.

The purpose of this paper is to explore the mechanism of experimental results given in [1,2], and to develop a theory on the physics of the mechanism so that the results can be properly interpreted and analyzed in depth. And this work certainly may lead to a concept for developing electromagnetic radiation sources based on the combination of electronics and photonics and the nanotechnique as well, especially for frequencies higher than terahertz (THz).

This paper makes a detailed theoretical exploration of the mechanism of the light well [1]. In Sec. II is the general theoretical formulation to derive the expression of the incident fields for diffraction radiation. Section III presents the theory of the waveguide with nanoscale periodic structure and obtains the dispersion equation of the structure. The theory of a beam-wave interaction is shown in Sec. IV to prove that the light-well mechanism [1] does not belong to the beam-wave interaction. The theory of the diffraction radiation of the nanoscale periodic structure excited by the electron beam is given in Sec. V, and the numerical calculations are shown in Sec. VI. The results given in Secs. V and VI confirm that the light-radiation mechanism is a special kind of diffraction radiation excited by the electron beam in a waveguide with a periodical structure. Finally, Sec. VII presents the conclusion and discussion.

II. GENERAL THEORETICAL FORMULATION

For an electron beam uniformly moving in a smooth cylindrical waveguide, a space-charge wave can be excited and sustained. The space-charge wave is a slow wave closely accompanying the electron beam, and it cannot radiate. The influence of the waveguide only leads to the "reduction factor" to the space-charge wave (decreases the plasma frequency of the electron beam) [3–5]. Therefore the electron beam cannot excite the guided TE and TM modes in a smooth cylindrical waveguide. The charged particles or electron bunch also cannot excite the guided modes in a smooth waveguide, only the local field moving together with them can be excited [6,7].

*hu_m@uestc.edu.cn

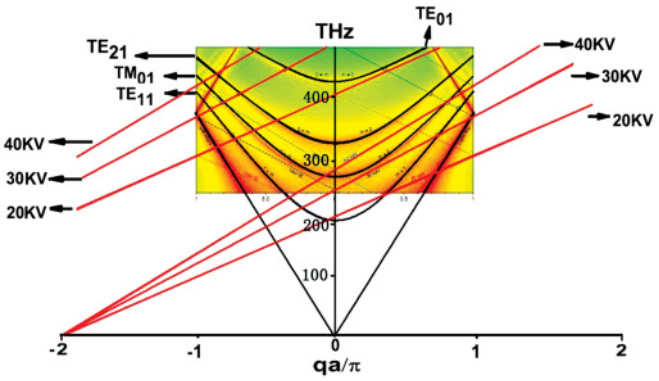

FIG. 1. (Color online) Brillouin diagram of the guided modes of infinite periodic cylindrical gold cavity with a radius of 350 nm expanded from Fig. 3 in [1], where 1 eV = 241.5 THz. The **a** means period and **q** is the longitude wave vector. The guided modes are TE_{11}, TM_{01}, TE_{21}, TE_{01} and TM_{11} modes (the last two modes are degenerate modes).

Now we are going to deal with the mechanism problem and we will show that in a cylindrical waveguide with periodic structure, the diffraction radiation can be excited as the guided modes propagating along the waveguide. The general theoretical formulation is given below. The scheme to be studied is shown in Fig. 2.

First, we should derive the expressions of the incident fields for diffraction radiation. To do so, the following inhomogeneous Helmholtz equation is used:

$$\frac{1}{r}\frac{\partial}{\partial r}\left(r\frac{\partial E_z}{\partial r}\right)+\frac{1}{r^2}\frac{\partial^2 E_z}{\partial \theta^2}+\frac{\partial^2 E_z}{\partial z^2}-\frac{1}{c^2}\frac{\partial^2 E_z}{\partial t^2}=j\omega\frac{4\pi}{c}J_z. \tag{1}$$

The current density J_z can be expressed as

$$J_z=qu_0\frac{\delta(r-r_0)}{r}\delta(\theta-\theta_0)\delta(z-u_0t), \tag{2}$$

where a uniformly moving electron beam is injected into the waveguide at the point (r_0,θ_0) with velocity u_0 and charge quantity q.

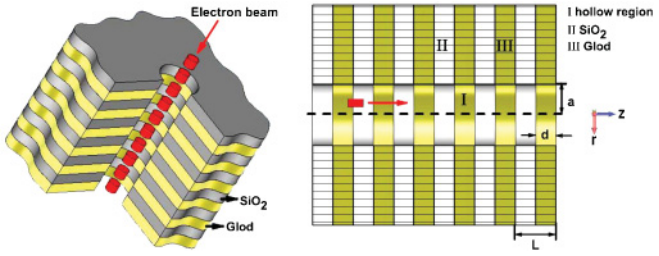

FIG. 2. (Color online) Schematic model of the light well to be studied in this paper. It can either be open or closed in the radiation direction.

Substituting Eq. (2) into Eq. (1) and making use of the Fourier transformation, Eq. (1) can be transformed into the expression in the frequency domain:

$$\frac{1}{r}\frac{\partial}{\partial r}\left(r\frac{\partial E_z}{\partial r}\right)+\left(k_c^2-\frac{m^2}{r^2}\right)E_z = -j2k_0q\frac{\delta(r-r_0)}{r}e^{jm(\theta-\theta_0)}e^{jk_z^iz}, \tag{3}$$

where $k_c^2=k_0^2-k_z^{i\,2}$, $k_z^i=\omega/u_0$, $k_0=\omega/c$, m (integer) denotes the azimuthal variation number of the field, and ω is angular frequency.

Making use of the integral transformation, the Bessel-Fourier series expansion, and the Wronskian approach, Eq. (3) can be solved and the frequency component of the incident field of the electron beam can be obtained:

$$E_z^i=-\pi k_0q\sum_m^\infty H_m^{(1)}(k_cr)J_m(k_cr_0)e^{jm(\theta-\theta_0)+jk_z^iz}, \quad r\geqslant r_0,$$
$$E_z^i=-\pi k_0q\sum_m^\infty H_m^{(1)}(k_cr_0)J_m(k_cr)e^{jm(\theta-\theta_0)+jk_z^iz}, \quad r\leqslant r_0, \tag{4}$$

where $J_m(k_cr)$ and $H_m^{(1)}(k_cr)$ are the first kind of Bessel function and Hankel function of the mth order, respectively. Here, the wave factor $e^{-j\omega t}$ is ignored.

The theory given above is a general one, and for the symmetrical mode ($m=0$), we get

$$E_z^i=-\pi k_0qH_0^{(1)}(k_cr)J_0(k_cr_0)e^{jk_z^iz}, \quad r\geqslant r_0,$$
$$E_z^i=-\pi k_0qH_0^{(1)}(k_cr_0)J_0(k_cr)e^{jk_z^iz}, \quad r\leqslant r_0. \tag{5}$$

For the case of no electron beam injection, it is just for the periodic electrodynamic system, so we only need to let $q=0$, and Eq. (3) becomes the homogeneous equation

$$\frac{1}{r}\frac{\partial}{\partial r}\left(r\frac{\partial E_z}{\partial r}\right)+\left(k_{ch}^2-\frac{m^2}{r^2}\right)E_z=0, \tag{6}$$

where $k_{ch}^2=k_0^2-k_z^2$, $k_z=\omega/v_p$, and v_p is the phase velocity of the fundamental wave. Solving this equation, the diffraction radiation in the structure can be obtained, and the solutions will be given in the following sections.

Now we get the longitudinal electric fields excited by the electron beam. Making use of the Maxwell equations, transverse fields can be expressed in terms of the longitudinal fields as

$$E_t=\frac{jk_z}{k_0^2\epsilon_r-k_z^2}\nabla_tE_z,$$
$$H_t=\frac{-jk_0\epsilon_r}{k_0^2\epsilon_r-k_z^2}e_z\nabla_tE_z. \tag{7}$$

For the case of TM modes $H_z=0$, all the electromagnetic fields induced by the electron beam in the structure can be obtained.

Therefore making use of the general theoretical formations [Eqs. (4) and (5)], the theoretical exploration of the light-well mechanism will be developed in the following sections.

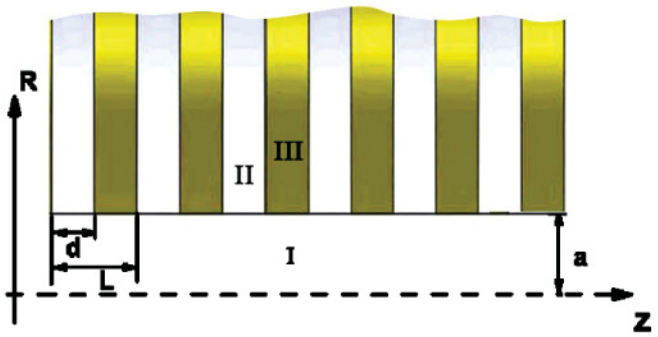

FIG. 3. (Color online) Scheme of the waveguide with nanoscale periodic structure. Three regions are shown: region I is the cylindrical hole; region II is SiO_2 filling; and region III is gold. The period is L, the width of region II is d, and a is the radius.

III. THEORY OF THE WAVEGUIDE WITH NANOSCALE PERIODIC STRUCTURE

Before dealing with the mechanism of the light radiation observed in [1], the waveguide with periodic structure should be studied [8]. The scheme and structural parameters with which we are now concerned are shown in Fig. 3. The scheme has three regions: I. the hollow region; II. the dielectric (SiO_2 filling) region, $nL \leqslant z \leqslant nL + d$; and III. the gold region $nL + d \leqslant z \leqslant (n+1)L$, $n = 0,1,2,3,\ldots$, while L is the period, and d is the thickness of gold layers, $d = L/2$. We can see that region II (SiO_2 filling) is a radial transmission line, and the waves are propagating along each line as transverse electromagnetic (TEM) waves, since the width of the gap is much smaller than the wavelength. The light-well nanoscale structure is made of gold and the operation wavelength is around 710 nm, so SPs should be taken into account. The permittivity of the gold can be expressed as $\epsilon_r^{\mathrm{III}} = 1 - \omega_p^2/(\omega^2 - j\omega\gamma)$ according to Dude's model [9]. Under this consideration, the expressions of the fields in different regions can be obtained by solving the homogeneous Eq. (6). The fields in region I can be expressed as (we only consider the TM modes with azimuthally symmetric case, see Sec. V)

$$\begin{aligned} E_z^I &= \sum_{n=-\infty}^{+\infty} A_n J_0(k_{cn} r) e^{jk_{zn} z}, \\ H_\theta^I &= \sum_{n=-\infty}^{+\infty} A_n \frac{jk_0}{k_{cn}} J_1(k_{cn} r) e^{jk_{zn} z}, \end{aligned} \tag{8}$$

where $J_0(k_{cn}r)$ and $J_1(k_{cn}r)$ are the first kind of Bessel function of zeroth and first order, respectively, and $k_{cn}^2 = k_0^2 - k_{zn}^2$, $k_{zn} = k_z + 2n\pi/L$. Here, the Bloch-Flouquet theorem has been used to satisfy the periodical boundary condition.

The electromagnetic fields in region II (SiO_2 filling region) are

$$\begin{aligned} E_z^{\mathrm{II}} &= BK_0(k_{cs} r), \\ H_\theta^{\mathrm{II}} &= -\sqrt{\varepsilon_r^{\mathrm{II}}} BK_1(k_{cs} r), \end{aligned} \tag{9}$$

where $k_{cs} = jk_0\sqrt{\varepsilon_r^{\mathrm{II}}}$, and $\varepsilon_r^{\mathrm{II}}$ is the relative permittivity of the SiO_2 filling.

In region III (gold region), with the SPs taken into consideration, the EM fields are

$$\begin{aligned} E_z^{\mathrm{III}} &= CK_0(k_{ct} r), \\ H_\theta^{\mathrm{III}} &= -\sqrt{\varepsilon_r^{\mathrm{III}}} CK_1(k_{ct} r), \end{aligned} \tag{10}$$

where $k_{ct} = jk_0\sqrt{\varepsilon_r^{\mathrm{III}}}$, and $\varepsilon_r^{\mathrm{III}}$ is the relative permittivity of the gold as shown previously.

Using the boundary condition, the dispersion equation of the nanoscale structure with SPs taken into account can be obtained:

$$\begin{aligned} P \sum_{n=-\infty}^{+\infty} \frac{K_0(k_{ct}a)M_2}{J_0(k_{cn}a)L} J_1(k_{cn}a)M_3 &= Q\frac{k_{cn}\varepsilon_r^{\mathrm{II}}}{k_{cs}} K_1(k_{cs}a)d \\ &\quad + Q \sum_{n=-\infty}^{+\infty} \frac{K_0(k_{cs}a)M_1}{J_0(k_{cn}a)L} J_1(k_{cn}a)M_3, \end{aligned} \tag{11}$$

where

$$P = \sum_{n=-\infty}^{+\infty} \frac{K_0(k_{cs}a)M_1}{J_0(k_{cn}a)L} J_1(k_{cn}a)M_4,$$

$$\begin{aligned} Q = \sum_{n=-\infty}^{+\infty} \frac{K_0(k_{ct}a)M_2}{J_0(k_{cn}a)L} J_1(k_{cn}a)M_4 \\ + \frac{k_{cn}\varepsilon_r^{\mathrm{III}}}{k_{ct}} K_1(k_{ct}a)(L-d), \end{aligned}$$

$$M_1 = d\sin c\left(\frac{k_{zn}d}{2}\right)e^{-jk_{zn}\frac{d}{2}}, \quad M_2 = -j\frac{e^{-jk_{zn}L} - e^{-jk_{zn}d}}{k_{zn}},$$

$$M_3 = d\sin c\left(\frac{k_{zn}d}{2}\right)e^{jk_{zn}\frac{d}{2}}, \quad M_4 = j\frac{e^{jk_{zn}L} - e^{jk_{zn}d}}{k_{zn}}.$$

The above series is convergent.

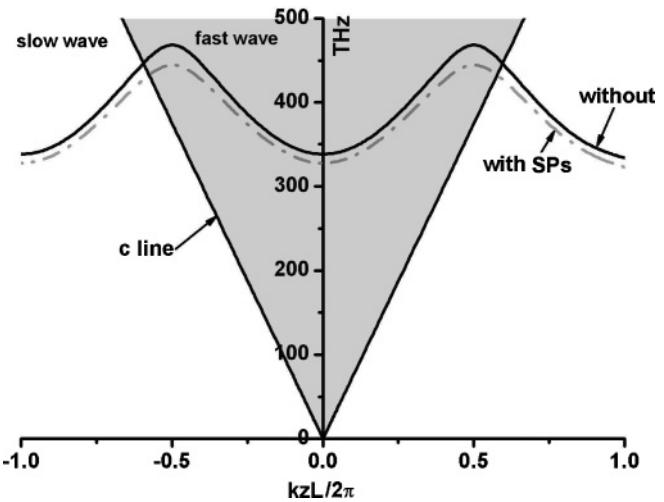

FIG. 4. Calculated dispersion curves of the TM_{01} mode of the structure shown in Fig. 3 at radius $a = 375$ nm, period $L = 400$ nm and $d = 200$ nm. The calculations are carried out with SPs (dashed line) and without SPs (solid line) taken into account. The shaded regions are the fast waves, while outer regions are slow waves.

In Eq. (11), if we assume $\varepsilon^{\mathrm{III}} \to -\infty$, we get the dispersion equation without SPs:

$$\sum_{n=-\infty}^{+\infty} \frac{K_0(k_{cs}a)M_1}{k_{cn}J_0(k_{cn}a)L} J_1(k_{cn}a)M_3 + \frac{\varepsilon_r^{\mathrm{II}}}{k_{cs}} K_1(k_{cs}a)d = 0. \quad (12)$$

By numerically calculating Eqs. (11) and (12), we can obtain the dispersion curves of the guided modes with and without taking SPs into consideration. The results are shown in Fig. 4.

From Fig. 4 we can see that not only fast waves but also slow waves can exist in the waveguide with periodic structure, which is different from the case of a smooth waveguide as shown in Fig. 1. Figure 4 also shows that the influence of SPs tends to slightly decrease the cutoff frequency of the guided mode. It can be understood that once SPs are excited, the skin depth of the gold should be taken into account which will enlarge the radius of the waveguide in effect. The skin depth can be calculated by the expression of $\delta = \frac{\lambda}{2\pi}\frac{\sqrt{\epsilon'+1}}{\epsilon'}$ [9]. For the wavelength range around 700 nm, the skin depth in the gold is about 42 nm.

IV. BEAM-WAVE INTERACTION

At first, we need to make sure if the electron beam-wave interaction can be considered as the mechanism of light radiation in [1]. Making use of the Maxwell equations and boundary conditions [10,11], the dispersion equation of the interaction between the electron beam and the guided mode in the waveguide with periodic structure can be obtained as follows:

$$\frac{-1}{k_{cn}} \sum_{n=-\infty}^{+\infty} \left(\frac{K_0(k_{ct}a)e^{\alpha_z d/2}(M_1+M_2)}{[I_0(k_{c3n}a)\chi_{1n} + K_0(k_{c3n}a)\chi_{2n}]L} + \frac{\varepsilon_r^{\mathrm{III}}}{\varepsilon_r^{\mathrm{II}}} \frac{K_0(k_{cs}a)\sin c\left(\frac{k_{zn}d}{2}\right)d}{[I_0(k_{c3n}a)\chi_{1n} + K_0(k_{c3n}a)\chi_{2n}]L} \right)$$

$$\times [I_1(k_{c3n}a)\chi_{1n} - K_1(k_{c3n}a)\chi_{2n}] \sin c\left(\frac{k_{zn}p}{2}\right) p = \frac{\varepsilon_r^{\mathrm{III}}}{k_{cs}} K_1(k_{cs}r)(2e^{\alpha_z d/2}M_3 + d), \quad (13)$$

where

$$\alpha_z^2 = \left(\varepsilon_r^{\mathrm{II}} - \varepsilon_r^{\mathrm{III}}\right)k_0^2, \quad M_1 = \frac{e^{-(\alpha_z + jk_{zn})\frac{d}{2}} - e^{-(\alpha_z + jk_{zn})\frac{p}{2}}}{\alpha_z + jk_{zn}}, \quad M_2 = \frac{e^{(-\alpha_z + jk_{zn})\frac{p}{2}} - e^{(-\alpha_z + jk_{zn})\frac{d}{2}}}{-\alpha_z + jk_{zn}}, \quad M_3 = \frac{e^{-\alpha_z d/2} - e^{-\alpha_z p/2}}{\alpha_z},$$

$$\chi_1 = \frac{[I_0(k_{c2n}r_2)G_1 + K_0(k_{c2n}r_2)G_2]\,K_1(k_{c3n}r_2) + \frac{k_{c3n}\varepsilon_2}{k_{c2n}\varepsilon_3}K_0(k_{c3n}r_2)\,[I_1(k_{c2n}r_2)G_1 - K_1(k_{c2n}r_2)G_2]}{I_0(k_{c3n}r_2)K_1(k_{c3n}r_2) + I_1(k_{c3n}r_2)K_0(k_{c3n}r_2)},$$

$$\chi_2 = \frac{[I_0(k_{c2n}r_2)G_1 + K_0(k_{c2n}r_2)G_2]\,I_1(k_{c3n}r_2) - \frac{k_{c3n}\varepsilon_2}{k_{c2n}\varepsilon_3}I_0(k_{c3n}r_2)\,[I_1(k_{c2n}r_2)G_1 - K_1(k_{c2n}r_2)G_2]}{K_0(k_{c3n}r_2)I_1(k_{c3n}r_2) + K_1(k_{c3n}r_2)I_0(k_{c3n}r_2)},$$

$$G_{1n} = \frac{I_0(k_{c1n}r_1)K_1(k_{c2n}r_1) + \frac{(k_{c2}\varepsilon_1)}{(k_{c1}\varepsilon_2)}K_0(k_{c2n}r_1)I_1(k_{c1n}r_1)}{I_0(k_{c2n}r_1)K_1(k_{c2n}r_1) + I_1(k_{c2n}r_0)K_0(k_{c2n}r_1)}, \quad G_{2n} = \frac{K_0(k_{c2n}r_1)I_1(k_{c2n}r_1) + K_1(k_{c2n}r_1)I_0(k_{c2n}r_1)}{I_0(k_{c1n}r_1)I_1(k_{c2n}r_1) - \frac{(k_{c2}\varepsilon_1)}{(k_{c1}\varepsilon_2)}I_1(k_{c1n}r_1)I_0(k_{c2n}r_1)},$$

where r_1 and r_2 are the inner and the outer radius of the electron beam, respectively, and $p = L - d$. Also, $k_{c1n} = k_{c3n} = \sqrt{-(\frac{\omega}{c})^2 + k_{zn}^2}, k_{c2n} = \sqrt{-(\frac{\omega}{c})^2(1 - \omega_p^2/\omega^2) + k_{zn}^2}, \varepsilon_1 = \varepsilon_3 = 1$, and $\varepsilon_2 = 1 - \omega_p^2/\omega^2$, here ω_p is the plasma angular frequency $\omega_p^2 = \frac{\rho_0 e}{m_0\varepsilon_0}$, and m_0 is the electron mass and ρ_0 is the beam density.

By solving the above dispersion equation, the growth rate of the beam-wave interaction can be obtained [12]. The numerical calculations of this dispersion equation show that in order to get the light radiation with frequency around 400 THz, the starting current density should be larger than 10^7 A/cm^2. This value is much beyond the state of the art of cathode technology. As a matter of fact, in the experiments of [1] the current density is only 700 A/cm^2 which is far from enough to excite the interaction to generate light radiation. Therefore, the results given above lead to the conclusion that the light radiation observed in [1] does not belong to the mechanism of beam-wave interaction.

V. DIFFRACTION RADIATION IN THE WAVEGUIDE WITH NANOSCALE PERIODIC STRUCTURE

It is essential to find the mechanism of the light radiation detected in [1]. It is well known that besides the beam-wave interaction, there are the following mechanisms of the radiation excited by a uniformly moving electron beam: Cherenkov radiation, Smith-Purcell radiation, and transition radiation [13,14]. Cherenkov radiation has nothing to do with the light radiation concerned here. Smith-Purcell and transition radiations were mentioned in [1]. However, Smith-Purcell radiation is in an open free space and its dispersion relation can be expressed as

$$\lambda = -\frac{L}{n}\left(\frac{1}{\beta} - \cos\theta\right), \quad (14)$$

where λ is the wavelength of the diffraction radiation, n is the order of the harmonics, $\beta = u_0/c$ is the relative velocity, and θ is the radiation angle from the electron moving direction

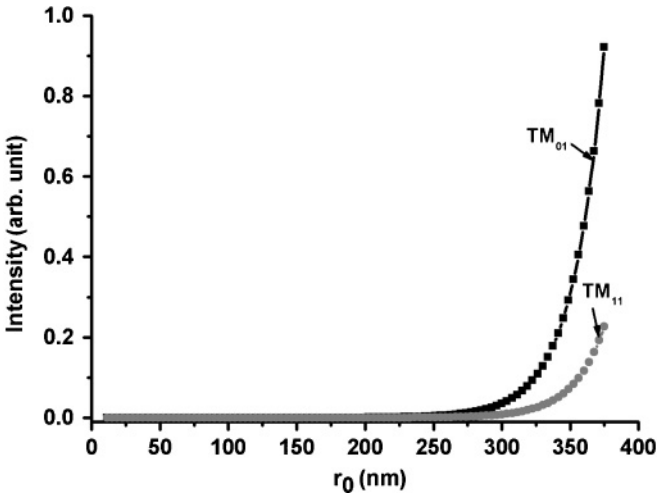

FIG. 5. Incident wave intensity of TM_{01} mode (black square line) and TM_{11} mode (gray circle line).

[15–17]. Equation (14) shows that the radiation frequency depends on both the order of harmonics and the radiation angle. It is obvious that the light radiation observed in experiments in [1] is not the Smith-Purcell radiation. As for transition radiation, it also has frequency-angle dependence in the open free space. In general it requires at least hundreds of periods and rather high (above MeV) energy of the electron beam [18,19]. So the light radiation observed in [1] cannot belong to transition radiation either.

The above discussion indicates that there must be an alternative mechanism for the light radiation detected experimentally in [1]. Therefore we will explore the mechanism of the diffraction radiation in the light well next.

When the electron beam is injected into the waveguide with nanoscale periodic structure the incident wave will be induced. And this incident wave has to propagate along the waveguide as the guided mode. It would appear that when the electron beam is injected at the point (r_0,θ_0), the preferable mode to be excited is the TM_{11} mode. But in fact, the fundamental mode TM_{01} is much easier to be excited. We can see that phenomenon in Fig. 5, which shows that the intensity of the incident wave of the TM_{01} mode is much higher than that of the TM_{11} mode.

Therefore only the mode of TM_{01} needs to be considered in detail. Based on Eqs. (1) and (4) in Sec. II, we can get the analytical expression of the incident wave induced by the electron beam:

$$\begin{aligned} E_z^i &= -\pi k_0 q H_0^{(1)}(k_c r) J_0(k_c r_0) e^{jk_z^i z}, \\ H_\theta^i &= j\frac{\pi k_0^2 q}{k_c} H_1^{(1)}(k_c r) J_0(k_c r_0) e^{jk_z^i z}. \end{aligned} \tag{15}$$

Then the diffraction radiation will be excited in the waveguide with periodic structure. These diffraction radiation waves also have to propagate along the waveguide as the guided modes. Obviously, only TM modes can be excited, and the TM_{01} mode is the dominant part.

So, the diffraction radiation in the waveguide with periodic structure should be expressed as

$$\begin{aligned} E_z^d &= \sum_{n=-\infty}^{+\infty} A_n J_0\left(k_{cn}^d r\right) e^{jk_{zn}^d z}, \\ H_\theta^d &= \sum_{n=-\infty}^{+\infty} \frac{jk_0}{k_{cn}^d} A_n J_1\left(k_{cn}^d r\right) e^{jk_{zn}^d z}. \end{aligned} \tag{16}$$

Here, the Bloch-Flouquet theorem has been used to satisfy the periodical boundary condition. And ${k_{cn}^d}^2 = k_0^2 - {k_{zn}^d}^2$, $k_{zn}^d = \omega/u_0 + 2n\pi/L$.

The fields in the region II (SiO_2 filling gaps) E_z^s, H_θ^s and region III (gold) E_z^g, H_θ^g can be written as

$$\begin{aligned} E_z^s &= BK_0(k_{cs} r), \\ H_\theta^s &= -\sqrt{\epsilon_r^{\mathrm{II}}} BK_1(k_{cs} r), \end{aligned} \tag{17}$$

$$\begin{aligned} E_z^g &= CK_0(k_{ct} r), \\ H_\theta^g &= -\sqrt{\epsilon_r^{\mathrm{III}}} CK_1(k_{ct} r). \end{aligned} \tag{18}$$

The coefficients A_n, B, C are determined by the incident fields of Eq. (15) together with the following boundary conditions:

$$E_z^i\big|_{r=a} + E_z^d\big|_{r=a} = \begin{cases} E_z^s\big|_{r=a}, & 0 < z < d, \\ E_z^g\big|_{r=a}, & d < z < L, \end{cases} \tag{19}$$

$$\begin{aligned} \int_0^d H_\theta^i dz\Big|_{r=a} + \int_0^d H_\theta^d dz\Big|_{r=a} &= \int_0^d H_\theta^s dz\Big|_{r=a}, \\ \int_d^L H_\theta^i dz\Big|_{r=a} + \int_d^L H_\theta^d dz\Big|_{r=a} &= \int_d^L H_\theta^g dz\Big|_{r=a}. \end{aligned} \tag{20}$$

Here, the coefficients A_n, B, and C in Eqs. (16)–(18) can be obtained:

$$\begin{aligned} A_n &= B\frac{K_0(k_{cs}a)M_1}{J_0(k_{cn}^d a)L} + C\frac{K_0(k_{ct}a)M_2}{J_0(k_{cn}^d a)L} - \frac{R_e}{J_0(k_{cn}^d a)L}, \\ B &= \frac{Q_2W_{11} - Q_1W_{22}}{W_{11}W_{22} - W_{21}W_{12}}, \quad C = \frac{Q_1W_{22} - Q_2W_{12}}{W_{11}W_{22} - W_{21}W_{12}}, \end{aligned} \tag{21}$$

where

$$W_{11} = \sum_{n=-\infty}^{+\infty} \frac{K_0(k_{ct}a)M_2}{k_{cn}^d J_0(k_{cn}^d a)L} I_1\left(k_{cn}^d a\right) M_3,$$

$$W_{12} = \sum_{n=-\infty}^{+\infty} \frac{K_0(k_{cs}a)M_1}{k_{cn}^d J_0(k_{cn}^d a)L} J_1\left(k_{cn}^d a\right) M_3 + \frac{\varepsilon_r^{\mathrm{II}}}{k_{cs}} K_1(k_{cs}a)d,$$

$$W_{21} = \sum_{n=-\infty}^{+\infty} \frac{K_0\left(k_{ct}a\right)M_2}{k_{cn}^d J_0(k_{cn}^d a)L} J_1\left(k_{cn}^d a\right) M_4 + \frac{\varepsilon_r^{\mathrm{III}}}{k_{ct}} K_1(k_{ct}a)(L-d),$$

$$W_{22} = \sum_{n=-\infty}^{+\infty} \frac{K_0(k_{cs}a)M_1}{k_{cn}^d J_0(k_{cn}^d a)L} J_1\left(k_{cn}^d a\right) M_4,$$

$$Q_1 = \sum_{n=-\infty}^{+\infty} \frac{I_1(k_{cn}^d a)}{J_0(k_{cn}^d a) k_{cn}^d L} M_3 R_e + j\frac{1}{\omega\varepsilon} R_{h1},$$

$$Q_2 = \sum_{n=-\infty}^{+\infty} \frac{R_e}{J_0(k_{cn}^d a) k_{cn}^d L} J_1(k_{cn}^d a) M_4 + j\frac{1}{\omega\varepsilon} R_{h2},$$

$$R_e = -\pi k_0 q H_0^{(1)}(k_c a) J_0(k_c r_0) L,$$

$$R_{h1} = -\pi q d \frac{k_0^2}{k_c} H_1^{(1)}(k_c a) J_0(k_c r_0) \sin c\left(\frac{k_z^i d}{2}\right) e^{jk_z^i \frac{d}{2}},$$

$$R_{h2} = -\pi q \frac{k_0^2}{k_c} H_1^{(1)}(k_c a) J_0(k_c r_0) \frac{e^{jk_z^i d} - e^{jk_z^i L}}{k_z^i}.$$

Substitute Eq. (21) into Eqs. (16)–(18) and the diffraction radiation fields in the waveguide with periodic structure can be achieved. Integrating the Poynting vector along the cross section of the propagating region I, the output power of the diffraction radiation in the longitudinal direction can also be obtained:

$$P_z = \frac{1}{2} Re\left\{\iint E_r^r (H_\theta^r)^* r\, dr\, d\theta\right\}$$
$$= \frac{\pi}{2} \sum_n^{\infty} \frac{k_{zn}^d k}{k_{cn}^{d\,2}} |A_n|^2 \frac{a}{k_{cn}^d} \left\{k_{cn}^d a \left[J_0(k_{cn}^d a)\right]^2 - 2J_0(k_{cn}^d a) J_1(k_{cn}^d a) + k_{cn}^d a \left[J_1(k_{cn}^d a)\right]^2\right\}. \quad (22)$$

Equation (22) shows that the total output power is the sum of that from the fundamental wave and all space harmonics. It can be seen from Eq. (22) that the output power is proportional to $|A_n|^2$, and $|A_n|$ is proportional to the beam current. So, in principle, Eq. (22) is the special form of the kinetic power theorem [20,21], which governs the balance of the energy of electromagnetic radiation and the electron beam in general.

VI. NUMERICAL CALCULATIONS

To verify that the mechanism of the light radiation detected in the experiment of [1] is just the diffraction radiation in the waveguide with periodic structure excited by the electron beam as shown in Sec. V, the results of numerical calculations should agree with those of experiments. Now we will deal with this in this section.

Figure 6 shows the calculated dispersion curve of the TM_{01} mode of the light well and the harmonics of the electron beam lines with different energies. We can see that each harmonic of the electron beam has the intersection point ($A_{0,-1,-2,\ldots}$ and $B_{0,-1,-2,\ldots}$, etc., shown in the figure) with the corresponding harmonic branch of the dispersion curve. Based on the analysis in Sec. V, these intersection points are the coupling points of the diffraction radiation with the guided modes (TM_{01} mode). We can see from the figure that the frequency and direction of the diffraction radiation can all be determined by these points. So we call them "working points" hereinafter.

From Fig. 6, we can also see that for the electron beam with certain energy, the diffraction radiation frequency and direction of all harmonics are the same. So the output power of diffraction radiation should be the sum of that from fundamental wave and all harmonics as indicated in Eq. (22).

The spectrums of the diffraction radiation can then be calculated based on Eq. (22) and the results are shown in Fig. 7. We can see that for the beam energy of 40, 35, 30, and 20 keV, the corresponding radiation peaks occur at the frequencies of 448, 432, 413, and 368 THz, respectively. These frequency peaks are very close to the experimental results of [1] except that the widths of the peaks are narrower. The reason for this discrepancy is due to the number of periods of the structure used in our theoretical analysis and that in the experiment of [1]. In our theoretical model, the period number is supposed to be infinity. Yet, in the experiment of [1], only six periods were used. It was indicated in [2] that the band width of the radiation peaks decrease with the increase of the period number. In this sense, the results we get by theoretical analysis are in good agreement with experimental results [1]. The working points in the dispersion curve of Fig. 6 show that all of these radiations are backward radiation which is the same as the experimental results. Figure 8 indicates that the calculated radiation intensity depends on the beam current and beam location r_0. We can see that the radiation intensity is

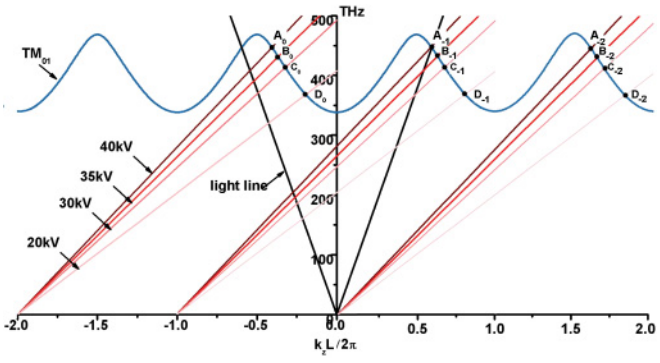

FIG. 6. (Color online) Brillouin diagram of dispersion curve (TM_{01} mode) of light-well structure with period $L = 400$ nm, radius $a = 375$ nm, and the electron beam lines with energies of 20, 30, 35, and 40 keV. The subscripts $0, -1, -2, \ldots$ of the coupling points indicate the order of the harmonics of the TM_{01} mode.

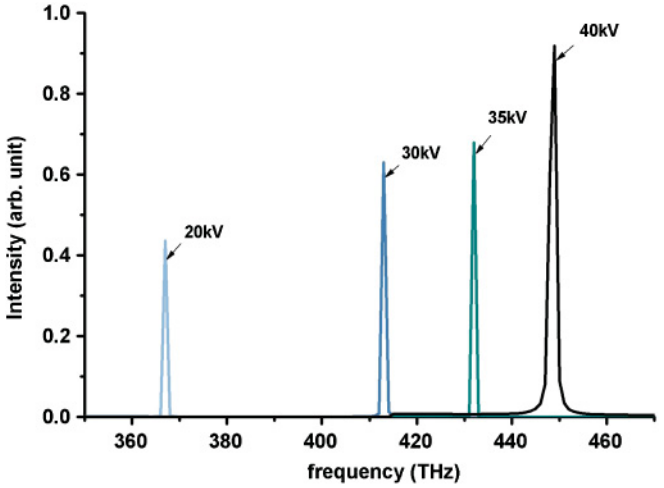

FIG. 7. (Color online) Diffraction radiation intensity exited by the electron beam with different energies.

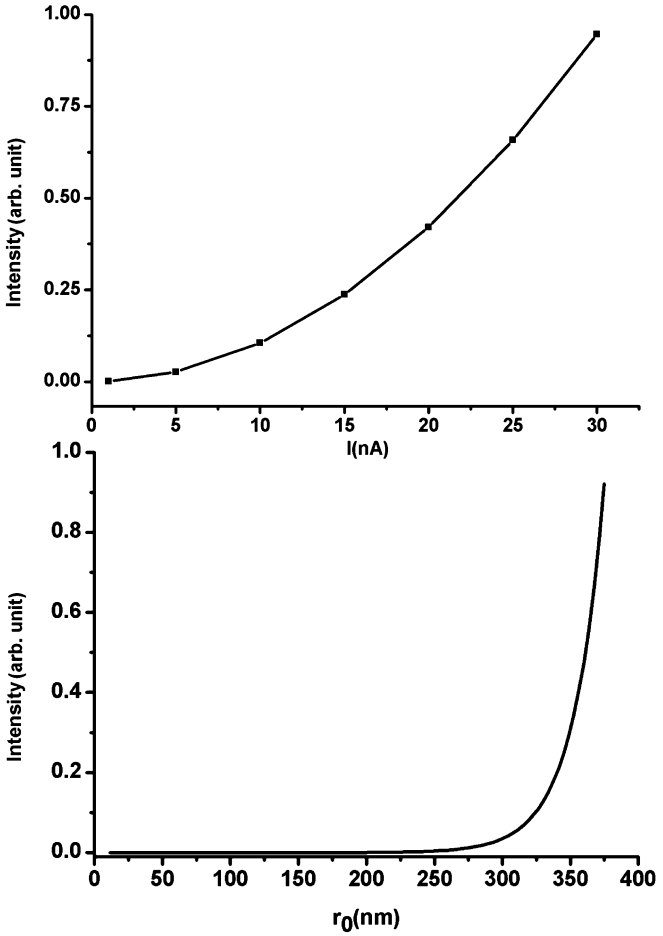

FIG. 8. (a) Radiation intensity vs current density. (b) Rdiation intensity vs beam location.

proportional to the square of the beam current density and the square of the modified Bessel function $[\,[I_0(|k_c|r_0)]^2]$ with the beam location. These results also agreed with the experimental results [1].

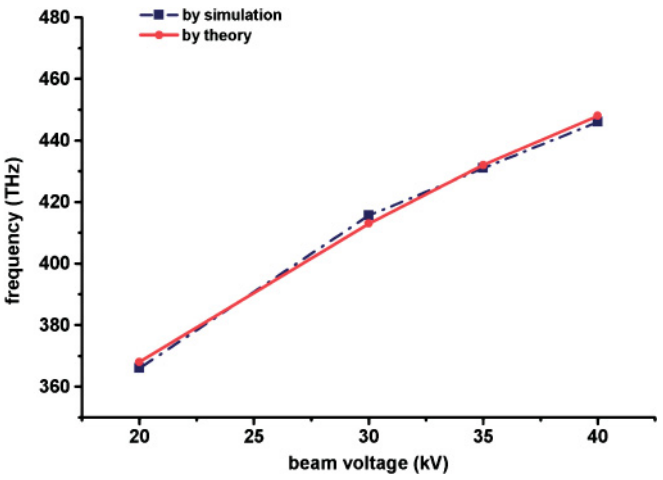

FIG. 9. (Color online) Frequency vs beam energy of the light radiation in the light well. It shows good agreement of the results of theoretical calculations (solid circle line) and those of digital simulation (dot-dash square line).

To verify the theoretical analysis, the digital simulations are also carried out to check the radiation frequency as shown in Fig. 9. We can see that the results of the numerical calculations and digital simulation agree with each other very well.

Our theoretical analysis is also valid for the model and size given in [2]. The results of numerical calculation based on our theory are in good agreement with those of the simulation [2].

VII. CONCLUSION AND DISCUSSION

Summarizing the detailed analysis and results in our paper, we confirm that the mechanism of light radiation in the light well [1] is a special kind of diffraction radiation in the waveguide with nanoscale periodic structure. The mechanism of this kind of diffraction radiation can be characterized as below:

(1) It does not require the electron beam current density to be higher than the starting current density. That means this kind of diffraction radiation can work at any value of current density.

(2) The diffraction radiation can be either fast wave or slow wave, and its direction can be either forward or backward. The characteristics of the radiation are determined by the working points on the dispersion curve of the waveguide with periodic structure.

(3) The diffraction radiation is from the whole guided mode including the fundamental wave and all space harmonics.

The requirement of the starting current density is one of the principal bases in traditional vacuum electronics and becomes a crucial problem of the development of higher frequency radiation sources for not only light radiation but also THz radiation. As known, THz science and technology are developing rapidly for there are many important and interesting potential applications [22–27]. However, developing the desired THz radiation sources and devices is still an urgent problem, although a variety of approaches have been researched [28–32]. To combine photonics, electronics, and nanotechnology might be a promising effort. Early in the 1990s, it was suggested to use quantum dots or wires to form an array to interact with the electron beam to generate THz radiation shown in Fig. 1 of [33]. However, this approach has not been successful yet. The special kind of mechanism of diffraction radiation presented in this paper together with advanced nanotechnology will greatly push forward the development of THz radiation sources.

To conclude: a special kind of diffraction mechanism has been presented and detailed theoretical exploration has been carried out, and the results of the numerical calculations and the digital simulation are in good agreement with that given in the experiments [1]. This kind of diffraction radiation is of significance in physics, optics, and THz science and technology.

ACKNOWLEDGMENTS

Authors extend their sincere thanks to Prof. Isabelle Yu for her kind help and comments. This work is supported by

the National Key Program of Fundamental Research of China under Contract No. 2007CB310401, and the National Natural Science Foundation of China under Contracts No. 10676110, No. 10911120058, and No.61001031.

[1] G. Adamo, K. F. MacDonald, N. I. Zheludev, Y. H. Fu, C.-M. Wang, D. P. Tsai, and F. J. García de Abajo, Phys. Rev. Lett. **103**, 113901 (2009).
[2] G. Adamo, K. F. MacDonald, Y. H. Fu, D. P. Tsai, F. J. García de Abaj, and N. I. Zheludev, J. Opt. **12**, 024012 (2010).
[3] S. Ramo, Phys. Rev. **56**, 276 (1939).
[4] G. Branch and T. Mihran, IRE Trans. Electron Devices **2**, 3 (1955).
[5] L. Shenggang, Y. Yang, M. Jie, and D. M. Manos, Phys. Rev. E **65**, 036411 (2002).
[6] V. V. G. Miano, L. Verolino, Nuovo Cimento B **111**, 659 (1996).
[7] R. S. ELLIOTT, *Electromagnetism* (McGraw-Hill, New York, 1966).
[8] I. Tigelis, J. Vomvoridis, and S. Tzima, IEEE Trans. Plasma Sci. **26**, 922 (1998).
[9] R. Heinz, *Surface Plasmons on Smooth and Rough Surfaces and on Gratings* (Springer-Velag, Berlin, 1988).
[10] Y. Zhang, M. Hu, Y. Yang, R. Zhong, and S. Liu, J. Phys. D **42**, 045211 (2009).
[11] M. Hu, Y.-X. Zhang, Y. Yan, R.-B. Zhong, and S.-G. Liu, Chin. Phys. B **18**, 3877 (2009).
[12] J. A. Swegle, J. W. Poukey, and G. T. Leifeste, Phys. Fluids **28**, 2882 (1985).
[13] P. A. Čerenkov, Phys. Rev. **52**, 378 (1937).
[14] V. Ginzburg, Phys. Usp. **39**, 973 (1996).
[15] S. J. Smith and E. M. Purcell, Phys. Rev. **92**, 1069 (1953).
[16] T. Takahashi, Y. Shibata, F. Arai, K. Ishi, T. Ohsaka, M. Ikezawa, Y. Kondo, T. Nakazato, S. Urasawa, R. Kato *et al.*, Phys. Rev. E **48**, 4674 (1993).
[17] A. S. Kesar, Phys. Rev. ST Accel. Beams **13**, 022804 (2010).
[18] V. Ginzburg and I. Frank, Zh. Eksp. Teor. Fiz. **16**, 15 (1946).
[19] M. L. Cherry, G. Hartmann, D. Müller, and T. A. Prince, Phys. Rev. D **10**, 3594 (1974).
[20] L. J. Chu, in IRE Annual conference on Electron Tube Research, 1951 (unpublished).
[21] W. H. Louisell, *Coupled Mode and Parametric Electronics* (Wiley, New York, 1960).
[22] R. Kohler, A. Tredicucci, F. Beltram, H. E. Beere *et al.*, Nature (London) **417**, 156 (2002).
[23] C. A. Schmuttenmaer, Terahertz Sci. Technol.**1**, 1 (2008).
[24] A. Doria, G. P. Gallerano, E. Giovenale, G. Messina, and I. Spassovsky, Phys. Rev. Lett. **93**, 264801 (2004).
[25] M. v. Ortenberg, Terahertz Sci. Technol. **1**, 9 (2008).
[26] P. Siegel, IEEE Trans. Microw. Theor. Tech. **50**, 910 (2002).
[27] M. Thumm, Terahertz Sci. Technol. **3**, 1 (2010).
[28] S. E. Korbly, A. S. Kesar, J. R. Sirigiri, and R. J. Temkin, Phys. Rev. Lett. **94**, 054803 (2005).
[29] Q. Hu, Terahertz Sci. Technol. **2**, 120 (2009).
[30] H. Eisele, Terahertz Sci. Technol. **3**, 109 (2010).
[31] S. Liu, M. Hu, Y. Zhang, Y. Li, and R. Zhong, Phys. Rev. E **80**, 036602 (2009).
[32] L. Shenggang, Z. Yaxin, H. Min, Y. Yang, and Z. RenBin, in *Infrared and Millimeter Waves, 2007 and the 2007 15th International Conference on Terahertz Electronics. IRMMW-THz. Joint 32nd International Conference on* (2007), pp. 899–900.
[33] S. A. Mikhailov and N. A. Savostianova, Appl. Phys. Lett. **71**, 1308 (1997).